



BRCA1 and BARD1 mediate apoptotic resistance but not longevity upon mitochondrial stress in *Caenorhabditis elegans*

Alessandro Torgovnick^{1,2,3,†}, Alfonso Schiavi^{1,4,†}, Anjumara Shaik^{1,‡}, Henok Kassahun^{5,6,‡}, Silvia Maglioni¹, Shane L Rea⁷, Thomas E Johnson⁸, Hans C Reinhardt², Sebastian Honnen⁹, Björn Schumacher³ , Hilde Nilsen^{5,6} & Natascia Ventura^{1,4,*} 

Abstract

Interventions that promote healthy aging are typically associated with increased stress resistance. Paradoxically, reducing the activity of core biological processes such as mitochondrial or insulin metabolism promotes the expression of adaptive responses, which in turn increase animal longevity and resistance to stress. In this study, we investigated the relation between the extended *Caenorhabditis elegans* lifespan elicited by reduction in mitochondrial functionality and resistance to genotoxic stress. We find that reducing mitochondrial activity during development confers germline resistance to DNA damage-induced cell cycle arrest and apoptosis in a cell-non-autonomous manner. We identified the *C. elegans* homologs of the BRCA1/BARD1 tumor suppressor genes, *brc-1/brd-1*, as mediators of the anti-apoptotic effect but dispensable for lifespan extension upon mitochondrial stress. Unexpectedly, while reduced mitochondrial activity only in the soma was not sufficient to promote longevity, its reduction only in the germline or in germline-less strains still prolonged lifespan. Thus, in animals with partial reduction in mitochondrial functionality, the mechanisms activated during development to safeguard the germline against genotoxic stress are uncoupled from those required for somatic robustness and animal longevity.

Keywords aging; apoptosis; BRC-1/BRD-1; DNA damage; mitochondria

Subject Categories Ageing; Autophagy & Cell Death; DNA Replication, Repair & Recombination

DOI 10.15252/embr.201845856 | Received 24 January 2018 | Revised 14 September 2018 | Accepted 26 September 2018 | Published online 26 October 2018
EMBO Reports (2018) 19: e45856

Introduction

Genomic integrity is maintained by the coordinated action of a plethora of genes that continuously survey the DNA to prevent the transmission of mutations to daughter cells either by temporarily halting the cell cycle and repairing the damage or by promoting apoptotic cell death. Deregulation of this finely controlled process leads to cancer, neurodegenerative diseases, and accelerated aging as clearly underlined by disorders ascribed to mutations in DNA surveillance genes [1,2]. Aging is a multifactorial process concurrently shaped by genetic and environmental factors and characterized by the progressive deterioration of cellular macromolecules and organelles with consequent functional decline of different tissues and organs, in turn leading to increased risk of contracting diseases and of death [3,4]. Resistance to infections and damaging agents declines with aging, and interventions that promote healthy aging are typically associated with increased resistance to different types of stressors. Emblematic examples of this aging trait have been extensively characterized in the genetically tractable model organism *Caenorhabditis elegans* (*C. elegans*) where lifespan-extending interventions were often identified in genetic screens for enhanced resistance to stress [5,6]. Paradoxically, reduced activity of core biological processes, such as mitochondrial metabolism, protein translation, the insulin/IGF signaling, and DNA repair, induces the expression of compensatory cellular stress responses, which are often causally involved in animal longevity and resistance to stress [7–10].

One class of *C. elegans* long-lived, stress-resistant mutants is defined by genetic or RNAi-mediated suppression of genes directly

1 Leibniz Research Institute for Environmental Medicine (IUF), Düsseldorf, Germany

2 Clinic I of Internal Medicine, Center for Integrated Oncology, Center for Molecular Medicine and the CECAD Research Center, University of Cologne, Cologne, Germany

3 Medical Faculty, Institute for Genome Stability in Aging and Disease, CECAD Research Center, University of Cologne, Cologne, Germany

4 Institute for Clinical Chemistry and Laboratory Diagnostic, Medical Faculty, Heinrich Heine University of Düsseldorf, Düsseldorf, Germany

5 Department of Clinical Molecular Biology, University of Oslo, Oslo, Norway

6 Akershus University, Akershus, Norway

7 Department of Pathology, University of Washington, Seattle, WA, USA

8 Institute for Behavioral Genetics & Department of Integrative Physiology, University of Colorado at Boulder, Boulder, CO, USA

9 Medical Faculty, Institute of Toxicology, Heinrich Heine University of Düsseldorf, Düsseldorf, Germany

*Corresponding author. Tel: +49 2113389203; E-mail: natascia.ventura@uni-duesseldorf.de

†These authors contributed equally to this work as first authors

‡These authors contributed equally to this work as second authors

or indirectly implicated in the functionality of the mitochondrial respiratory chain (MRC), the so-called mitochondrial mutants (*Mit* mutants) [11,12]. Changes in animal metabolism, the induction of protective and detoxifying systems (e.g., mtUPR, antioxidants, autophagy) [7,13–16], a smaller germline, a decreased but prolonged fertility, and a reduced adult size (often accompanied by slower development) are all associated with lifespan extension upon mitochondrial disturbance. Moreover, different molecular players have been identified in the past two decades that mediate *Mit* mutants' longevity: a handful of transcription factors [7,17–22], autophagy- and apoptosis-regulatory genes [7,14,18,23,24], some kinases [25–27], as well as some mitochondrial metabolites [28] and chromatin remodeling genes [29,30]. Nonetheless, whether the same molecular mechanisms underlie the different *Mit*-mutant's phenotypic features is largely unknown [14,31,32]. The *C. elegans* p53 ortholog, *cep-1*, specifies many of the *Mit*-mutant phenotypes, including animal's reduced fertility and germline size [14,17,18,33], and mediates germ-cell apoptosis in response to genotoxic stress [34,35]. However, whether pro-longevity mitochondrial stress affects systemic or germline resistance to genotoxic insults and whether these are simply associated or causally involved in animal extended longevity remain unexplored so far.

In this study, we addressed these questions and found that reducing mitochondrial activity not only reduces germ-cell proliferation and apoptosis in physiological conditions, but it also confers germline resistance to DNA damage-induced cell cycle arrest and apoptosis. This protective effect is not due to impaired apoptosis, whose activation and execution machinery are otherwise intact, but rather to improved DNA-damage detoxification and repair system. A small-scale RNAi screen revealed that an intact genome maintenance apparatus is indeed required to survive and specify *Mit*-mutant phenotypes and led to the identification of the *C. elegans* homologs of BRCA1 and BARD1 tumor suppressor genes (*brc-1* and *brd-1*, respectively) as mediators of the anti-apoptotic effect promoted by reducing mitochondrial activity. Unexpectedly, we found that the lifespan extension triggered by mitochondrial stress does not require *brc-1* and *brd-1* or other DNA-damage response (DDR) regulatory genes and is not paralleled by an improved systemic resistance to genotoxic insults. Of note, reducing mitochondrial function only in the germline was not sufficient to promote the anti-apoptotic effect while it still prolonged lifespan; on the other hand, reducing mitochondrial function only in the soma still protected the germline against genotoxic stress, but it actually curtailed lifespan. The uncoupled germline versus somatic responses elicited by a well-established lifespan-extending intervention indicates that genes which contribute to the conservation of the species do not segregate with the ones that promote longevity, a very sound process from an evolutionarily point of view.

Results

Pro-longevity mitochondrial stress reduces germline cell proliferation and apoptosis

The gonad of the *C. elegans* hermaphrodite is composed of two U-shaped tubes starting from their distal tip cell, the stem cell-like

compartment that gives rise to the mitotic zone. After a few rounds of proliferation, mitotic cells enter meiosis, become competent to undergo apoptosis, and differentiate into oocytes, which pass through the spermatheca to be fertilized. Embryos are subsequently laid through the vulva. The reduced germline size and fertility rate [36], associated with the extended lifespan of different *Mit* mutants, could then be ascribed to impaired germ-cell proliferation or to increased apoptosis (or both). To distinguish between these possibilities, we first quantified the number of mitotic and meiotic germ cells in animals with reduced expression of two MRC regulatory proteins, namely *frh-1*, the *C. elegans* ortholog of human frataxin (a mitochondrial protein involved in the biogenesis of iron–sulfur clusters, ISC), and *isp-1*, the ISC component of complex III of the MRC. *In vitro* germline staining with the fluorescent DNA intercalating agent DAPI (4',6-diamidino-2-phenylindole) revealed a significantly reduced number of mitotic and meiotic cells in long-lived *frh-1*- and *isp-1*-silenced animals compared to control animals (Figs 1A and B, and EV1A). In addition, *frh-1* and *isp-1* RNAi-treated animals also displayed a reduced number of germ cells positively stained for the G2/M-phase marker phospho-Ser10-histone 3 (PH3) and an increased number of germ cells expressing the cyclin-dependent kinase CDK-1, whose activity normally decreases to favor cell cycle progression through M-phase (Figs 1C and D, and EV5A and B). Moreover, in support of reduced but active germ-cell proliferation, *in vivo* pulse-chase experiments by feeding worms with bacteria incorporating EdU (5-ethynyl-2'-deoxyuridine), which reveal newly synthesized DNA, showed that mitochondrial stress significantly reduces the number of proliferating germ cells compared to wild-type animals (Figs 1E and EV5C).

We then quantified the number of apoptotic germ cells in physiological conditions and in response to different DNA-damaging agents. The number of apoptotic corpses in the germline of *frh-1* and *isp-1* RNAi-treated animals was significantly reduced under physiological conditions (Figs 1F and EV1B). Of note, silencing of mitochondrial genes also conferred resistance to apoptosis induced by different genotoxic stressors. Indeed, while as expected, the number of apoptotic corpses significantly accumulated in the gonad of wild-type animals after treatment with gamma radiation, UVC, cisplatin, or different doses of UVB, reducing mitochondrial functionality significantly prevented apoptotic induction in response to the applied DNA-damaging agents except cisplatin (Figs 2A–D and EV1B). Higher doses of UVB similarly arrested the development of both control and silenced animals (Fig EV1C).

Moderate mitochondrial stress promotes DNA-damage protective responses

The above-observed phenotypes in the germline of the *Mit* mutants may be ascribed to two completely opposite scenarios: either to an impairment of the DDR pathways (DNA-damage sensors/transducers or apoptotic machinery) [37,38] or to an improvement of DNA maintenance or damage avoidance/detoxification pathways activated by mild mitochondrial stress. The core apoptotic machinery in physiological conditions is executed by the consecutive roles of CED-9/*BCL2* (anti-apoptotic), CED-4/*APAF1*, and CED-3/*CASPASE* (pro-apoptotic proteins). In response to DNA damage, CED-9 is inactivated by the *cep-1* transcriptional induction of EGL-1 and CED-13, two BH3-only pro-apoptotic proteins. The recognition and

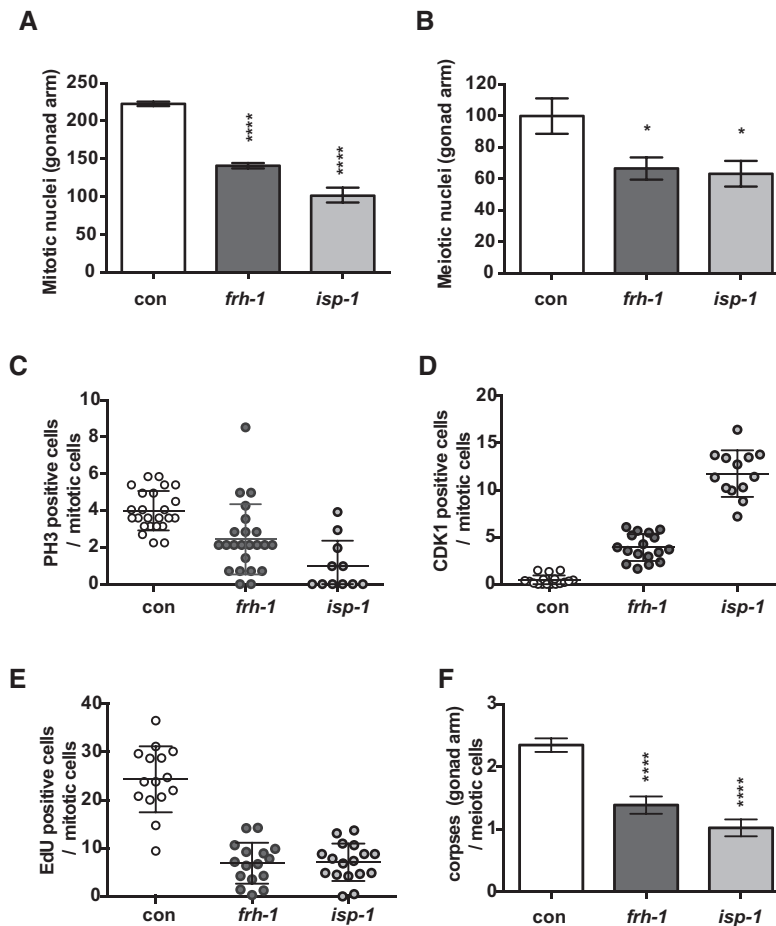


Figure 1. Pro-longevity mitochondrial stress reduces germ-cell proliferation and apoptosis in basal conditions.

A, B Quantification of mitotic (A) and meiotic (B) cells in the distal germline in wild-type animals fed bacteria transformed with either empty-vector (con) or vector-expressing dsRNA against *frh-1* (*frh-1*) or *isp-1* (*isp-1*).
C–E Quantification of dissected distal germline from wild-type animal stained either anti-phosphohistone H3 (anti-PH3) (C), anti-CDK-1 (anti-CDK-1) (D), or 5-ethynyl-2'-deoxyuridine (EdU—green) (E) relative to the total number of mitotic cells of wild-type animal.
F Average number of apoptotic corpses in the meiotic compartment relative to the total number of meiotic cells in wild-type worms fed as in (A).

Data information: Data are presented as mean \pm SEM (A, B, F) or as mean \pm SD (C–E). (A) $N = 3$ at least five worms per replicate and condition, (B) $N = 3$ at least 10 worms for condition (C–E) $N = 2$ at least five worms per replicate and condition, (F) $N = 5$ at least 10 worms per replicate and condition. * $P < 0.05$ and **** $P < 0.0001$ versus con (one-way ANOVA Tukey's multiple comparisons test).

final removal of the apoptotic corpses are then mediated by the transmembrane receptor CED-1. We thus assessed whether mitochondrial stress delays or compromises the apoptotic machinery. Time-course experiments clearly revealed that the apoptotic program is not simply delayed. Indeed, as expected, the number of apoptotic cells progressively increased at 12, 24, and 36 h after UVB treatment in wild-type young adults (24 h after L4 stage). However, upon *frh-1* and *isp-1* RNAi the number of apoptotic cells did not increase at any observed time point neither under physiological conditions nor in response to DNA damage (Fig 3A and B). The *ced-1(e1735)* engulfment mutant strain greatly facilitates the visualization of accumulating corpses. In support of an intact physiological apoptotic machinery, we found that apoptotic corpses accumulated normally in *frh-1* and *isp-1* RNAi-depleted *ced-1(e1735)* mutants, either during animal development or in the germline (Fig EV1D and E), thus also excluding that faster clearance could be the cause of reduced number of corpses. CED-9 represents a central regulator of

the apoptotic machinery in both basal and DNA damage-induced conditions. We observed that *ced-9(n1653ts)* loss-of-function mutants (which compared to a wild-type strain display an increased number of apoptotic corpses under physiological conditions) completely rescued the reduced physiological and DNA damage-induced apoptosis of *isp-1* and *frh-1* RNAi animals (Fig EV1F), a further indication that the apoptotic machinery at least downstream of *ced-9* is not impaired in response to mitochondrial stress. We then addressed whether the DNA-damage checkpoint activation upstream of *ced-9* is functional by quantifying the transcript levels of the two *cep-1* pro-apoptotic BH3 target genes in response to genotoxic stress. The expression of *egl-1* and *ced-13* was significantly induced in response to ionizing irradiation and UVB in both control and mitochondrial-stressed animals (Fig 3C–F), thus also revealing an intact *cep-1*-checkpoint activation.

Taken together, data shown so far indicate that pro-longevity mitochondrial stress reduces physiological and genotoxic stress-induced

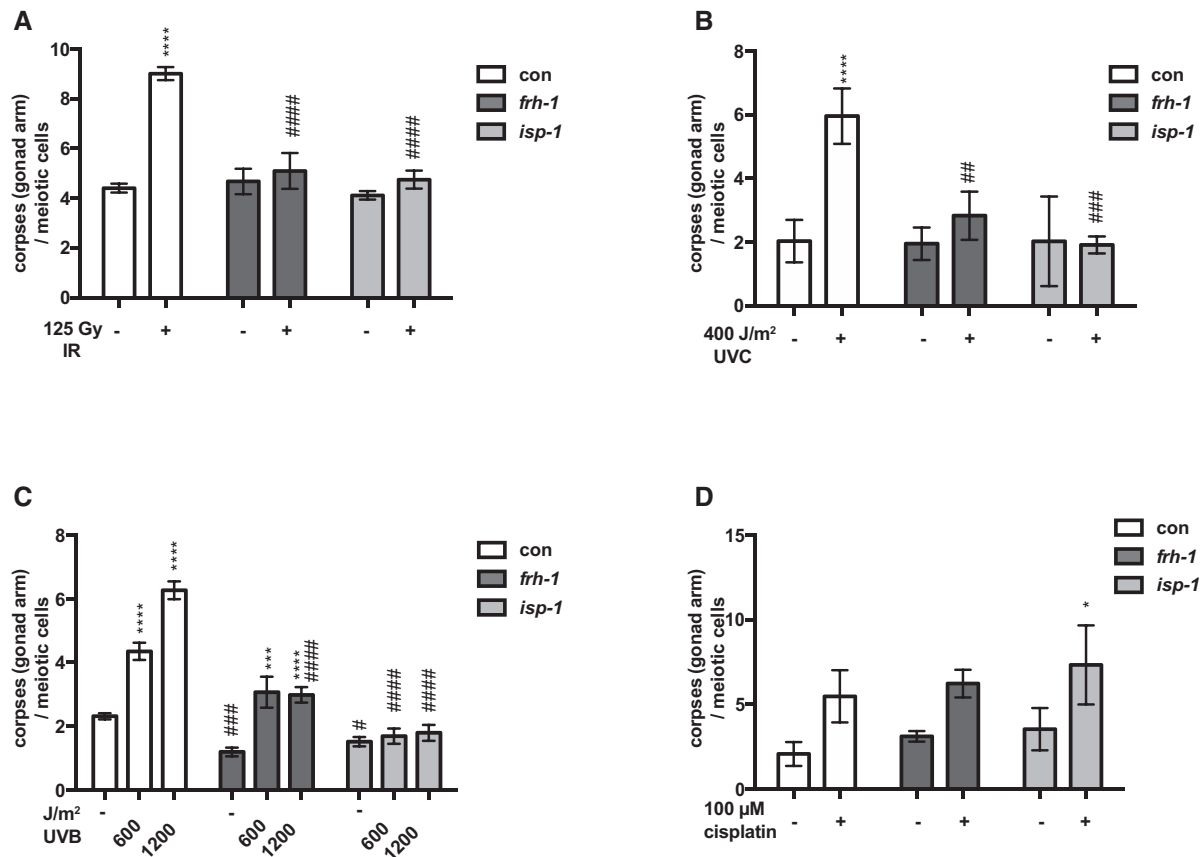


Figure 2. Mitochondrial stress protects against DNA damage-induced apoptosis.

A–D Quantification of apoptotic corpse in the meiotic compartment of *CED-1::GFP* (A, B, D) or wild-type strains (C) relative to the total number of meiotic cells, fed bacteria transformed with either empty-vector (con) or vector-expressing dsRNA against *frh-1* or *isp-1* and left untreated or treated with gamma radiation 125 Gy (A), UVC 400 J/m² (B), different doses of UVB (C), and 100 μM cisplatin.

Data information: Data are presented as mean ± SEM. For each panel at least *N* = 3 and 10 worms for replicate and condition. **P* < 0.05, ****P* < 0.001 and *****P* < 0.0001 versus untreated; #*P* < 0.05, ##*P* < 0.01, ###*P* < 0.001 and ####*P* < 0.0001 versus con. Not significant if nothing is specified. Two-way ANOVA Tukey's multiple comparisons test.

apoptosis without affecting neither the apoptotic machinery itself nor the DNA-damage checkpoint, thus most likely interfering with the upstream signaling required to recognize or repair the damage. Consistent with this scenario, we observed that, compared to wild-type animals, *frh-1*- and *isp-1*-silenced animals displayed reduced germline staining of the DNA-damage sensor PARP-1 under physiological conditions and an increased number of ionizing radiation-induced foci positive for replication protein A (RPA-1) and RAD-51, proteins that aid DNA-damage recognition and repair (Fig 4A and B). Of note, we found that the germ cells of *frh-1*- and *isp-1*-depleted animals were significantly resistant to radiation-induced arrest. Indeed, while UVB and gamma radiation reduced the number of mitotic cells in wild-type animals as expected, this reduction was only marginal or absent in response to *frh-1* or *isp-1* RNAi, respectively (Fig 4C and D). The ability to bypass a transient arrest in the germline of mitochondrial-perturbed animals was also reflected by the effect of *frh-1* and *isp-1* silencing to prevent p-histone-H3 reduction and CDK-1 increase upon gamma radiation as compared to their effect in control animals (Figs 5A and B, and EV5D and E). Interestingly, and as opposed to DNA-damage repair

mutants [39], whereas different types of genotoxic stress significantly reduced fecundity and fertility in wild-type animals, these were not as dramatically affected in *frh-1*- and *isp-1*-depleted animals (Fig 5C–H). These observations are in line with the notion that long-lived mutants are generally more resistant to different types of stressors and indicate that moderate mitochondrial disturbance increases resistance to radiation-induced germ-cell arrest and apoptosis possibly by promoting avoidance or detoxification/repair mechanisms in response to low level of transient replication stress or DNA damage. These mechanisms would, in turn, as opposed to DDR mutants, improve DNA maintenance and help animals cope with extrinsic genotoxic insults.

BRC-1/BRD-1 mediates the anti-apoptotic effect elicited by mitochondrial stress

To address this possibility, we carried out a small-scale genetic screen with the *isp-1(qm150); gst-4p::gfp* strain. Indeed, we have previously shown that the induction of the glutathione-S-transferase is an indirect readout for the activation of compensatory DNA-damage

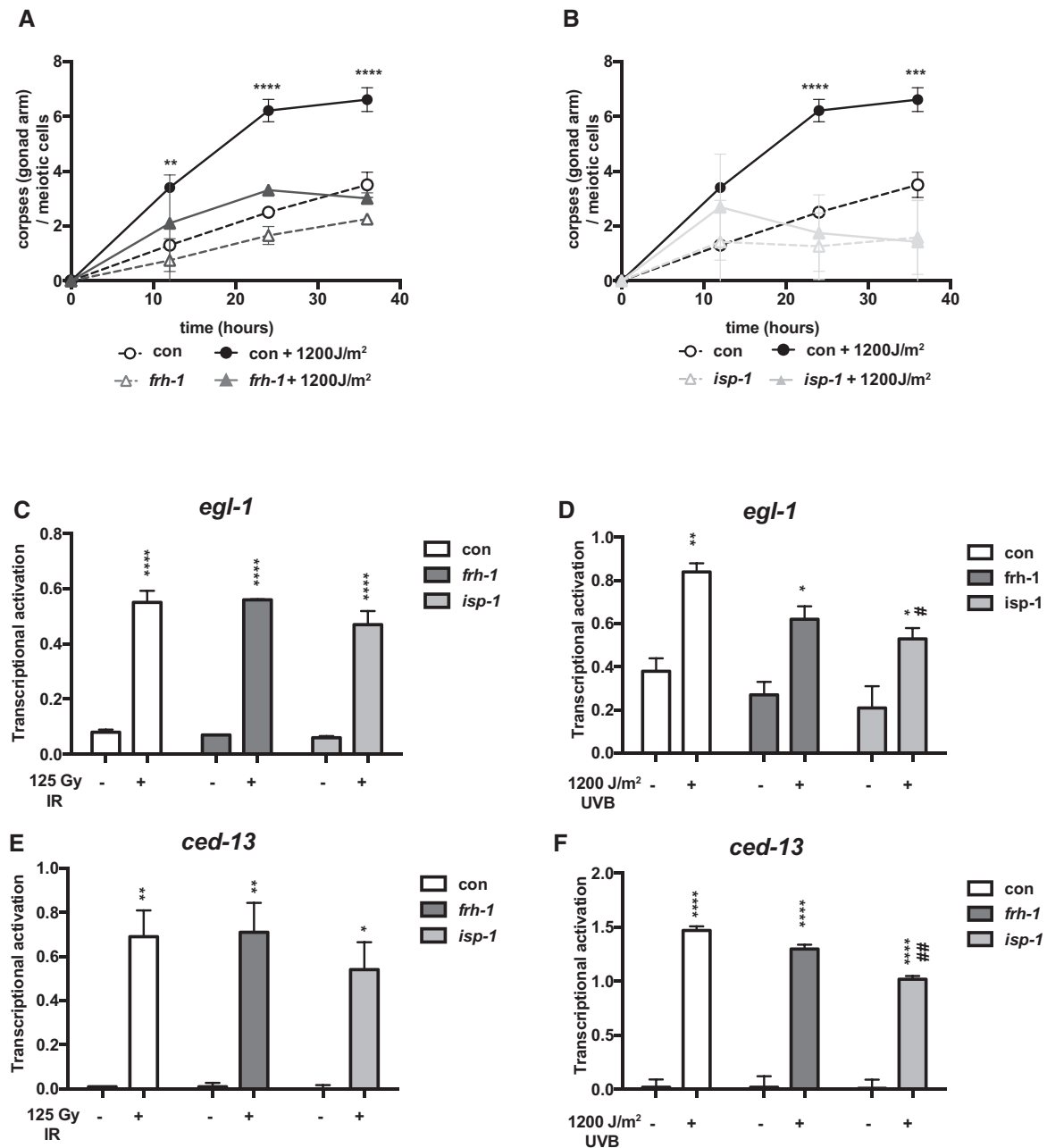


Figure 3. Mitochondrial stress does not impair the DNA-damage checkpoint.

A, B Time-course quantification of apoptotic corpses relative to the total number of meiotic cells from wild-type animals fed bacteria transformed with either vector-expressing dsRNA against *gfp* (con) or *frh-1* (A) or *isp-1* (B), and left untreated or exposed to 1,200 J/m² UVB. Apoptotic cells were counted 12, 24, and 36 h after exposure.

C–F Real-time PCR gene expression analysis of *egl-1* (C–D) and *ced-13* (E–F) genes, performed in wild-type animals fed bacteria transformed with either empty-vector (con) or with vector-expressing dsRNA against *frh-1* or *isp-1* and left untreated or treated with gamma radiation (C, E) or with UVB (D, F).

Data information: Data are presented as mean ± SEM, N = 3 (A, B) N = 2 (C, E), N = 4 (D, F). *P < 0.05, **P < 0.01, ***P < 0.001, and ****P < 0.0001 versus untreated; #P < 0.05 and ##P < 0.01 versus con. Not significant if nothing is specified. Two-way ANOVA Tukey's multiple comparisons test.

detoxification systems [40] and that *Mit* RNAi increases its expression, which is further induced by the lack of *cep-1* (the *C. elegans* p53 homolog) that concurrently suppresses *isp-1(qm150)* and *Mit* RNAi longevity [7,17,41]. Accordingly, we now crossed the *isp-1(qm150); gst-4p::gfp* strain with the *cep-1(gk138)* loss-of-function

allele and observed that the *gst-4* expression was further induced by the lack of *cep-1* in both wild-type and *isp-1* mutant animals (Fig EV2A). We thus exploited the *isp-1(qm150); gst-4p::gfp* along with its wild-type control strain, *gst-4p::gfp*, to screen ~250 RNAi clones against genes directly or indirectly involved in DNA

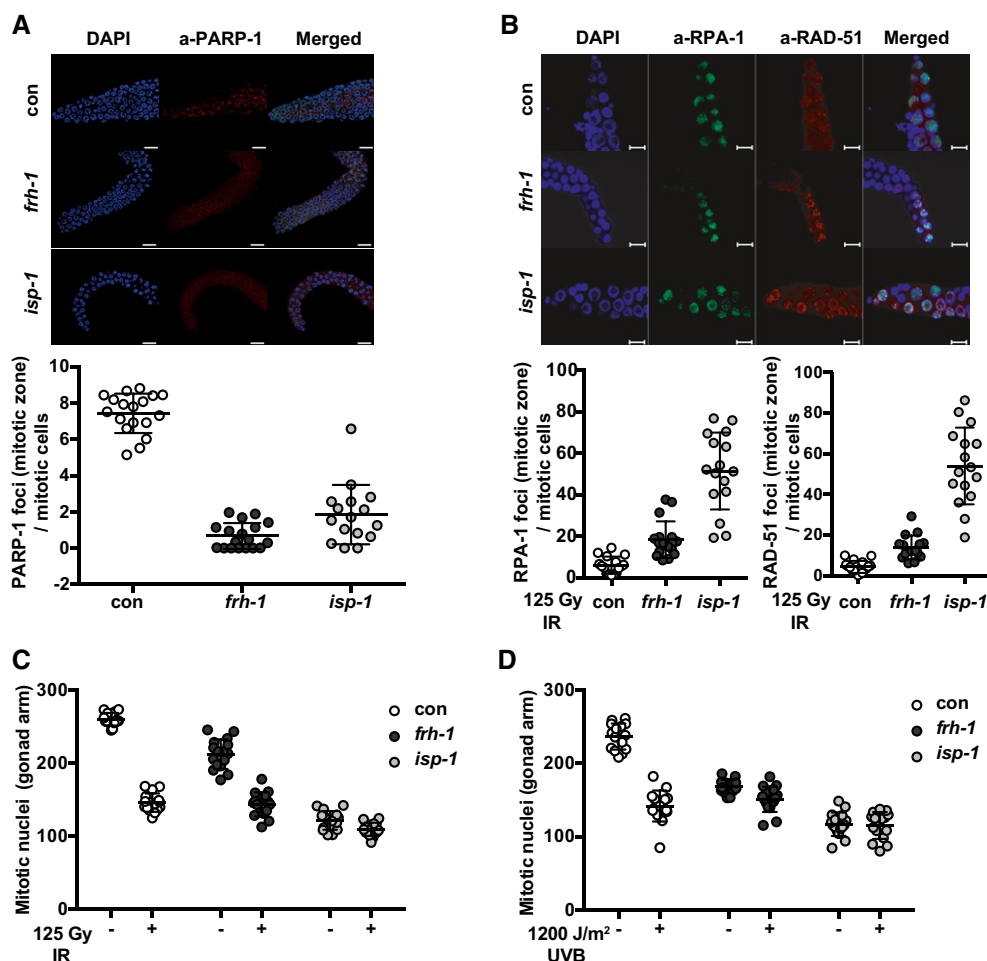


Figure 4. Mitochondrial-stressed animals overcome DNA-damage checkpoint.

A, B Representative fluorescence pictures and quantification (below the fluorescence pictures) of dissected adult gonads relative to the number of mitotic cells from wild-type animals fed bacteria transformed with either vector-expressing dsRNA against *gfp* (con) or *frh-1* and stained with DAPI (blue) and either anti-PARP-1 (red) (A) or anti-RPA-1 (green) and anti-RAD-51 (red) antibodies and treated with gamma radiation (125 Gy) (B) (untreated animals displayed no staining of RPA-1 and RAD-51, not shown). Scale bar: 20 μ m (A), 15 μ m (B).

C, D Quantification of mitotic cells in wild-type animals fed as (A) and left untreated or treated with gamma radiation 125 Gy (D) or with 1,200 J/m² UVB (E).

Data information: Data are presented as mean \pm SD. For each panel $N = 2, 8$ –10 worms per replicate and condition.

damage, repair, cell cycle, and chromatin organization (Fig EV2B; Appendix Table S1), to identify DNA protective genes promoted by pro-longevity mitochondrial stress. Different RNAi clones affected one of the observed phenotypes (viability, development, fertility, or *gst-4* expression) in both *isp-1(qm150)* and wild-type animals, and only a few uniquely affected *isp-1(qm150)* mutants either after one or two generations of feeding (Appendix Table S1 and S2). The identified clones did not similarly alter the different *isp-1* phenotypes, and the induction of the *gst-4* did not necessarily correlate with the alteration of a specific phenotypic change, implicating different molecular mechanisms in the regulation of fertility, development, and stress response of this long-lived mutant. Interestingly, while only a handful of clones rescued *isp-1*-delayed behaviors (development and/or egg lay rate) (e.g., *xpg-1*, *mms-19*, *rad-54*), the majority of them were actually synthetic lethal, leading to *isp-1*-arrested development (Appendix Table S2), thus revealing a central

requirement for genome maintenance pathways in mediating the protective cellular responses activated by mitochondrial stress.

We then turned to our screening results to identify a possible mediator of *Mit* mutants' resistance to genotoxic insults. Data shown so far are consistent with the possibility that the apoptotic block in response to mitochondrial stress resides between DNA-damage sensing and complete checkpoint activation. Thus, we decided to focus on *brc-1* and its partner gene *brd-1*, the orthologs of human *BRCA1* (the gene mutated in early-onset breast and ovarian cancers) and *BRCA1*-associating protein *BARD1*, respectively, which are required for a complete resolution of the checkpoint activation upon DNA damage-induced homologous recombination [42]. Silencing of *brc-1* consistently arrested development and increased *gst-4* expression only in *isp-1(qm150)*, while *brd-1* silencing had a less consistent lethal effect (Appendix Table S2). Although we could not reveal BRC-1 in total protein extracts from wild-type worms,

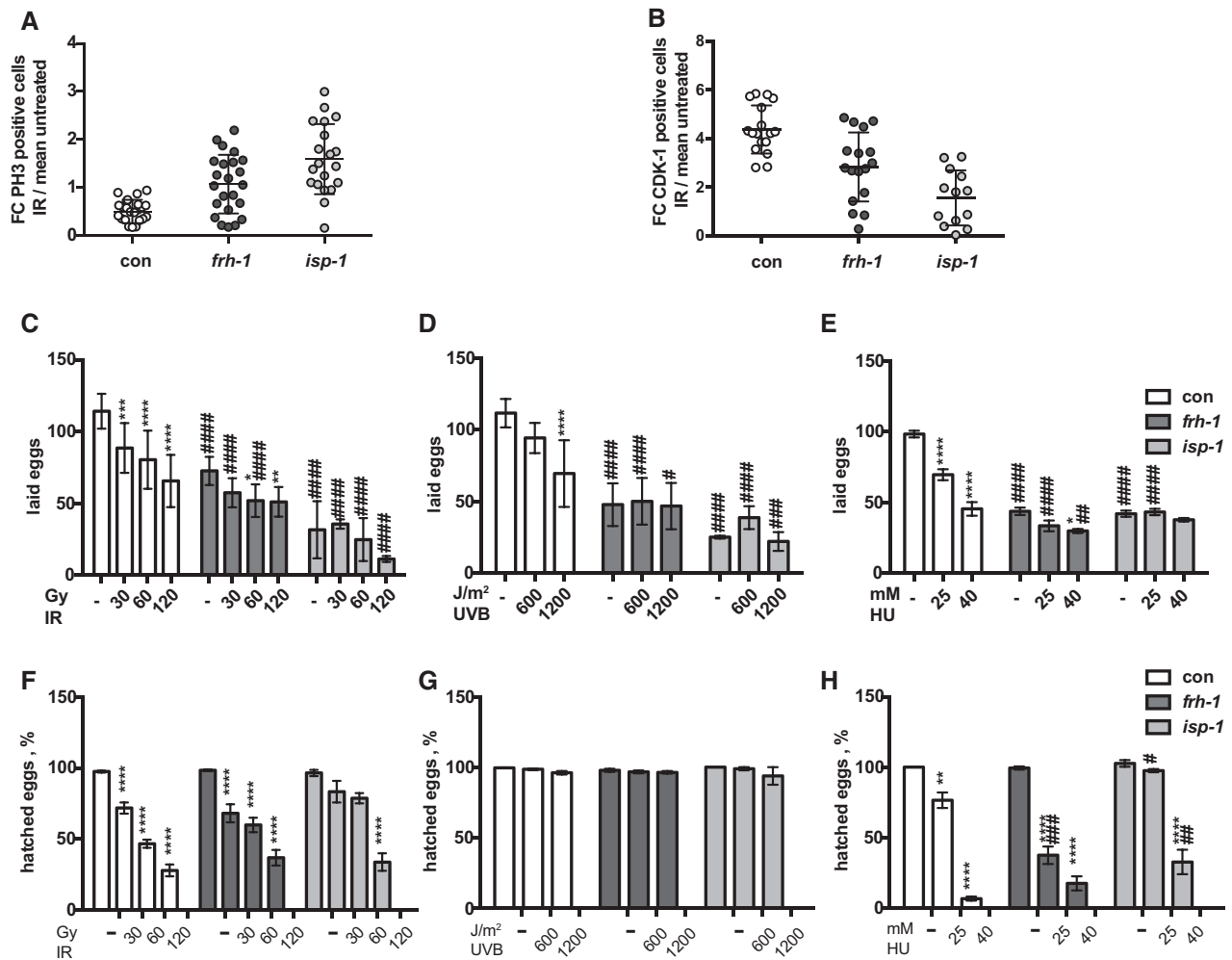


Figure 5. Moderate mitochondrial stress promotes DNA-damage protective responses.

A, B Quantification to the number of mitotic cells of dissected gonads from wild-type animals stained with either anti-phosphohistone H3 (anti-PH3) (A), anti-CDK-1 (CDK-1) (B) transformed with either empty-vector (con) or vector-expressing dsRNA against *frh-1* (*frh-1*) or *isp-1* (*isp-1*) and treated with gamma radiation 125 Gy. Quantification is expressed as fold changes of positive-stained cells treated over the positive untreated cells.

C–H Fertility (C–E) and fecundity (F–H) quantification of wild-type strain fed bacteria transformed with either empty-vector (con) or with vector-expressing dsRNA against *frh-1* or *isp-1*, and left untreated or treated with gamma radiation (C, F), UVB (D, G), or hydroxyurea (E, H) at the indicated doses.

Data information: Data are presented as mean ± SD (A, B) or as mean ± SEM (C–H). $N = 2$ (A, B), $N = 3$ (C–H) * $P < 0.05$, ** $P < 0.01$, *** $P < 0.001$ and **** $P < 0.0001$ versus untreated; # $P < 0.05$, ## $P < 0.01$, ### $P < 0.001$ and #### $P < 0.0001$ versus con. Not significant if nothing is specified. One-way ANOVA Tukey's multiple comparisons test (A, B); two-way ANOVA Tukey's multiple comparisons test (C–H).

there was a trend toward increased BRD-1 protein expression upon *frh-1* and *isp-1* RNAi, while gene expression analysis revealed an increase in *brc-1* following *frh-1* RNAi (Fig 6A and EV2C). Interestingly, while *brc-1(tm1145)* and *brd-1(gk297)* mutants did not affect the number of mitotic cells in *frh-1* or *isp-1* RNAi animals (Fig 6B), they completely prevented their ability to reduce apoptosis (Fig 6C). Of note, lack of *brc-1* or *brd-1*, which as expected increases the sensitivity to IR-induced germline apoptosis [42], also significantly increased the sensitivity of *frh-1* and *isp-1* RNAi animals to radiation-induced germ-cell apoptosis (Fig 6D). Yet, interestingly, mitochondrial disturbance still partially suppressed the high number of apoptotic cells in *brd-1* and *brc-1* mutants in response to IR (Figs 6D and EV2D) and *isp-1* RNAi could still protect *brc-1* mutants against UVB-induced apoptosis (Fig EV2E), suggesting the activation of

BRC/BRD-independent protective pathways [23]. In support of this possibility, we observed that, similar to the effect on wild-type animals, *frh-1* and *isp-1* RNAi also significantly prevented the drop in fertility induced by genotoxic stress in the *brc-1* and *brd-1* mutants (Fig EV3A and B) and partially rescued their embryonic lethality (Fig EV3C and D). Taken together, these results indicate that mitochondrial stress can induce both BRC/BRD-dependent and independent pathways regulating different DNA-damage responses.

Germline resistance to apoptosis is not involved in mitochondrial stress extension of lifespan

We then wondered whether germline resistance to apoptosis is causally involved in the lifespan extension elicited by *isp-1* and

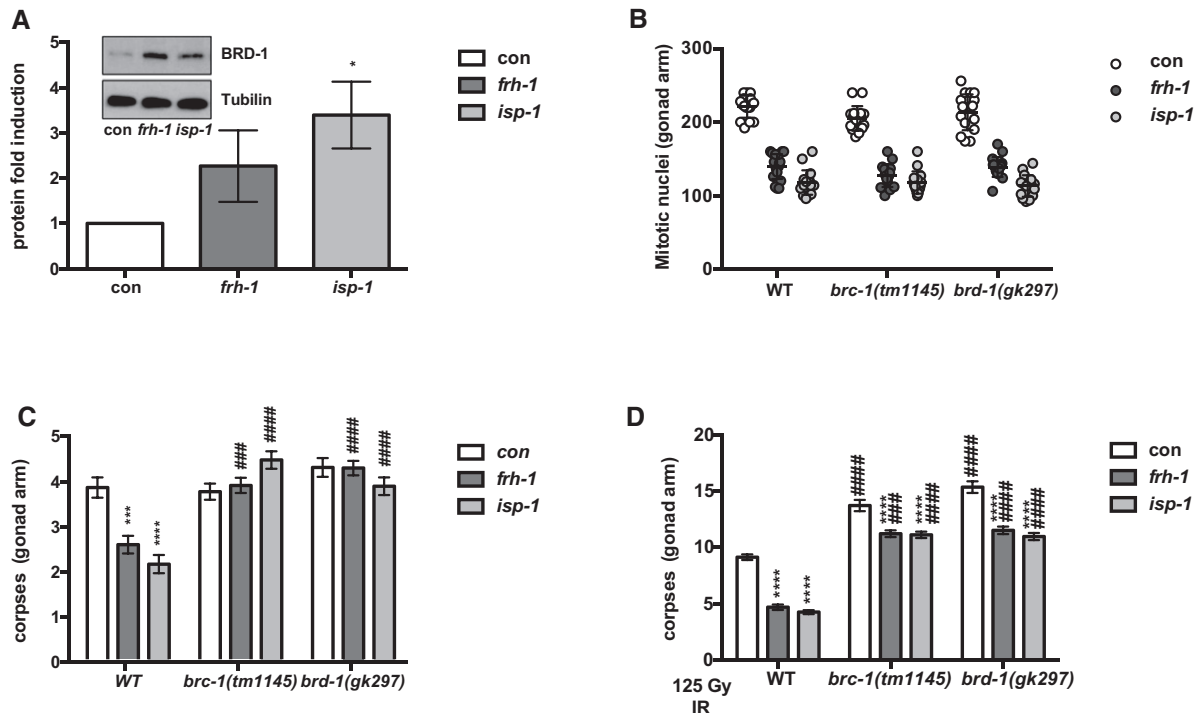


Figure 6. BRC-1/BRD-1-dependent and BRC-1/BRD-1-independent germline responses to mitochondrial stress.

A Quantification of BRD-1 protein and representative Western blot from wild-type worms fed bacteria transformed with either empty-vector (con) or with vector-expressing dsRNA against *frh-1* or *isp-1*.
B Quantification of mitotic nuclei in single gonad arm of wild-type (WT), *brc-1(tm1145)*, and *brd-1(gk297)* strains fed as in (A).
C, D Quantification of apoptotic corpse in wild-type (WT), *brc-1(tm1145)*, and *brd-1(gk297)* strains fed as in (A) and left untreated (C) or treated with ionizing radiation 125 Gy (IR) (D). Bar graphs are mean \pm SEM.

Data information: Data are presented as mean \pm SD $N = 2$ (A, B) or mean \pm SEM $N = 4$ (C, D), 8–10 worms per replicate and condition, * $P < 0.05$, *** $P < 0.001$, and **** $P < 0.0001$ versus untreated; ### $P < 0.001$ and #### $P < 0.0001$ versus con. Not significant if nothing is specified. Two-way ANOVA Tukey's multiple comparisons test (C–D).

frh-1 silencing. To this end, we assessed the lifespan of *ced-9* (*n1653ts*), *brc-1(tm1145)*, and *brd-1(gk297)* single mutants, which restored germ-cell apoptosis in response to mitochondrial stress, in control and mitochondrially disturbed animals. We found that *ced-9* loss of function significantly reduced lifespan in control animals as well as upon mitochondrial stress, bringing *frh-1* and *isp-1* RNAi lifespan back to wild-type levels, yet both *frh-1* and *isp-1* RNAi still significantly extended *ced-9* lifespan indicating *ced-9* only partially mediates their pro-longevity effect (Fig 7A; Table 1). The lifespan of *brc-1* and *brd-1* mutants was instead indistinguishable from that of wild-type animals, and, somewhat to our surprise, while *brc-1* and *brd-1* mutants significantly shortened and extended lifespan of *frh-1*-depleted animals, respectively, they did not affect the longevity of *isp-1* RNAi (Fig 7B and C; Table 1). The partial effect of loss of *ced-9* and the different effects of loss of *brc-1* or *brd-1* on *frh-1*- and *isp-1*-RNAi lifespans suggest that germline resistance to apoptosis is not causally involved in mitochondrial stress extension of lifespan. In support of a germline-independent pro-longevity effect, we also found that *isp-1* silencing can extend lifespan in germline-less strains (Fig 7D and E; Table 1). Moreover, we observed that the longevity of *isp-1* or *frh-1* RNAi animals was not abrogated by lack of most tested DNA maintenance genes that affected *isp-1*

mutant phenotypes (Fig EV4; Table 1) and that, contrary to their germline resistance to genotoxic stress, it was instead also negatively affected by UVB radiation, similarly to control animals. Specifically, the lifespan of control, *isp-1*, and *frh-1* RNAi animals treated as adults (1 day fertile) with 600–1,200–2,400 J/m² UVB was significantly shortened in a dose-dependent manner (Fig 7F–H; Table 1).

To further investigate systemic versus germline-specific effects elicited by mitochondrial stress, we finally assessed lifespan and radiation-induced apoptosis upon *isp-1* silencing only in the germline or in the soma. Interestingly, germline-specific *isp-1* RNAi still extended lifespan but not as much as in wild-type animals, while soma-specific RNAi actually curtailed lifespan (Fig 8A; Table 1) and did not reduce the size of *isp-1* RNAi-treated worms (Fig EV5F). On the other hand, unexpectedly, *isp-1* RNAi only in the germline did not protect against UVB-induced apoptosis, while soma-specific RNAi did it (Fig 8B). Altogether, our study indicates that in the *C. elegans* germline, the activation of the DDR following mitochondrial stress is a process uncoupled from the ones involved in animals longevity. Moreover, while upon MRC dysfunction a signal from the soma is required to promote germline protection against genotoxic stress, a pro-longevity signal from the soma and a lifespan-limiting signal from

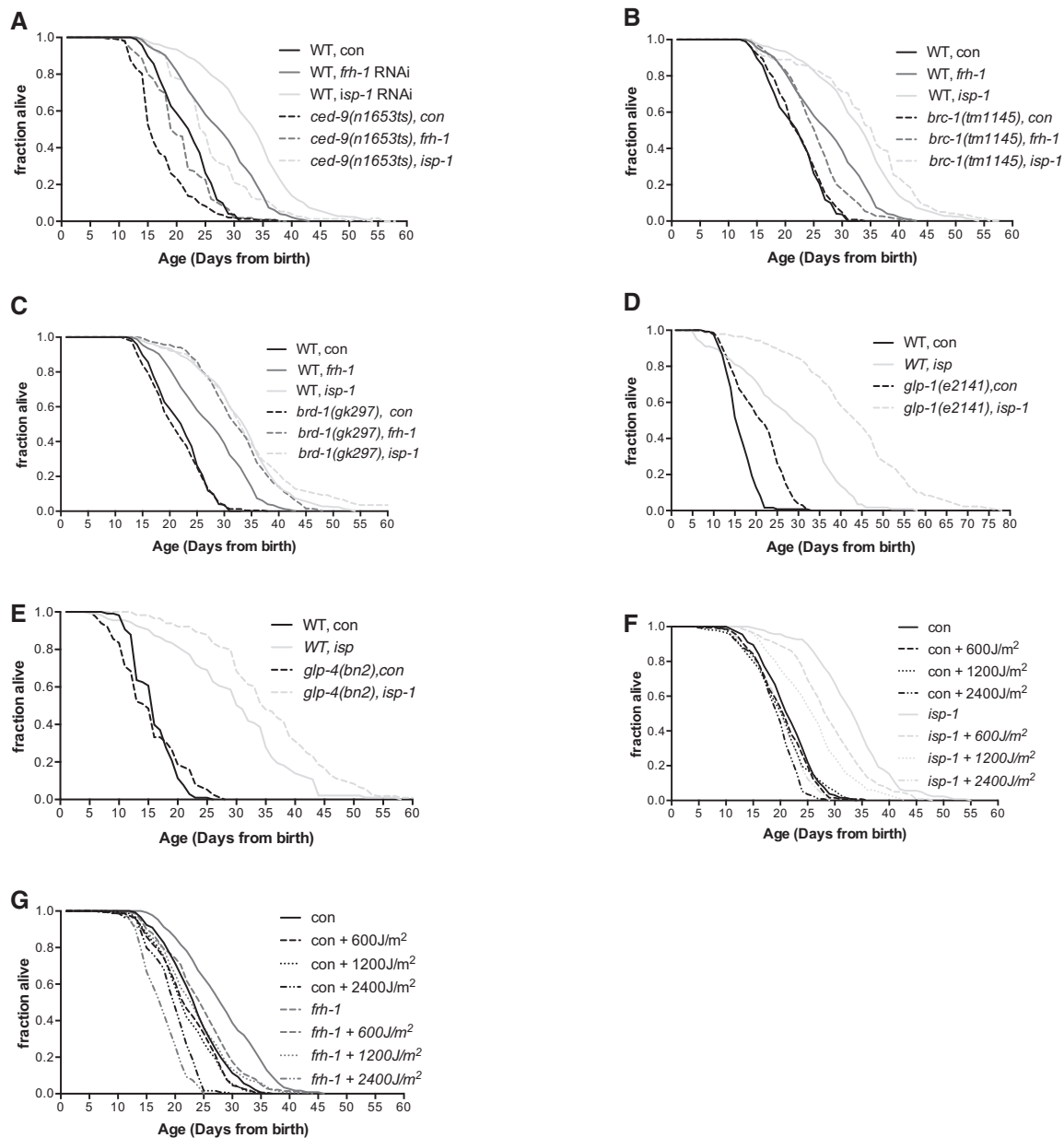


Figure 7. BRC-1 and BRD-1 do not mediate mitochondrial stress extension of lifespan.

A–E Kaplan–Meier survival curves of wild-type (WT) and *ced-9(n1653ts)* (A), *brc-1(tm1145)* (B), *brd-1(gk297)* (C), *glp-1(e2141)* (D), *glp-4(bn2)* (E), strains fed bacteria transformed with either empty-vector (con) or with vector-expressing dsRNA against *frh-1* or *isp-1*.

F, G Kaplan–Meier survival curves of wild-type animals fed bacteria transformed with either empty-vector (con) or with vector-expressing dsRNA against *isp-1* (F) or *isp-1* (G) and left untreated or treated with 600, 1,200, or 2,400 J/m² UVB. Comparison between curves was done using the log-rank test, and the summary of the statistic is reported in Table 1.

the germline cooperate for *Mit* mutants' lifespan extension (Fig 8C and D).

Discussion

In this study, we have shown for the first time that germline and somatic features in long-lived mitochondrial-perturbed animals are

mechanistically uncoupled. We observed that moderate mitochondrial stress reduces physiological germ-cell proliferation and apoptosis and provides germline protection against DNA damage-induced apoptosis, cell cycle arrest, and fertility drop. Most notably, we have identified BRC-1 and BRD-1 tumor suppressor genes as mediators of the anti-apoptotic effects against IR but not UVB, and not of animal's fertility or longevity, suggesting different mechanisms indeed mediate MRC dysfunction-associated phenotypes.

Table 1. Summary and statistical analysis of survival assays.

	Genotype	RNAi	Treatment	Mean lifespan	SE	P versus con/untreated	P versus wt	Sample size	Censor
Fig 7	Wild-type N2	con		19.0	0.3			320	31
		<i>frh-1</i>		24.6	0.5	<0.0001		320	86
		<i>isp-1</i>		30.1	0.5	<0.0001		240	23
	<i>ced-9(n1950)</i>	con		16.5	0.4		0.0002	220	71
		<i>frh-1</i>		19.6	0.5	<0.0001	<0.0001	220	113
		<i>isp-1</i>		25.1	0.8	<0.0001	<0.0001	160	75
	<i>brc-1(tm1145)</i>	con		19.5	0.3		NS	301	45
		<i>frh-1</i>		22.6	0.4	<0.0001	0.0012	297	111
		<i>isp-1</i>		31.4	0.8	<0.0001	NS	160	27
	<i>brd-1(gk297)</i>	con		18.4	0.3		NS	300	58
		<i>frh-1</i>		29.6	0.5	<0.0001	<0.0001	300	107
		<i>isp-1</i>		33.4	0.8	<0.0001	0.0073	160	17
	Wild-type N2	con		15.3	0.3			140	16
	(25°C)	<i>isp-1</i>		27.0	1.1	<0.0001		140	21
	<i>glp-4(bn2)</i>	con		19.9	0.5		<0.0001	140	6
	(25°C)	<i>isp-1</i>		42.3	1.2	<0.0001	<0.0001	140	8
	Wild-type N2	con		15.1	0.3			120	14
	(25°C)	<i>isp-1</i>		28.8	1.0	<0.0001		120	26
	<i>glp-1(e2141)</i>	con		14.4	0.6		NS	120	36
	(25°C)	<i>isp-1</i>		34.9	0.9	<0.0001	0.0003	120	8
	Wild-type N2	con	Untreated	22.8	0.4			160	18
		con	600 J/m ²	21.3	0.5	NS		165	10
		con	1,200 J/m ²	21.1	0.4	NS		165	14
		con	2,400 J/m ²	18.8	0.3	NS		160	29
		<i>frh-1</i>	Untreated	27.4	0.6		<0.0001	160	39
		<i>frh-1</i>	600 J/m ²	23.7	0.6	0.0002	0.001	158	20
		<i>frh-1</i>	1,200 J/m ²	22.5	0.6	<0.0001	NS	150	15
		<i>frh-1</i>	2,400 J/m ²	16.8	0.3	NS	0.0002	146	21
		con	Untreated	21.6	0.4			155	23
		con	600 J/m ²	20.7	0.4	NS		156	23
		con	1,200 J/m ²	20.4	0.5	NS		155	26
		con	2,400 J/m ²	19.4	0.4	NS		155	35
		<i>isp-1</i>	Untreated	33.4	0.6		<0.0001	155	28
		<i>isp-1</i>	600 J/m ²	29.2	0.6	0.0001	<0.0001	155	26
		<i>isp-1</i>	1,200 J/m ²	26.1	0.6	<0.0001	<0.0001	147	31
		<i>isp-1</i>	2,400 J/m ²	20.2	0.4	<0.0001	NS	153	24
Fig 8	Wild-type N2	con		19.7	0.4			205	17
		<i>isp-1</i>		23.6	0.4	<0.0001		198	9
	<i>rff-1(pl1417)</i>	con		18.5	0.4		NS	205	7
		<i>isp-1</i>		20.5	0.4	0.003	<0.0001	206	10
	<i>ppw-1(pk2505)</i>	con		24.5	0.5		<0.0001	207	73
		<i>isp-1</i>		20.8	0.6	<0.0001	0.002	202	148
Fig EV4	Wild-type N2	con		19.0	0.3			320	31
		<i>frh-1</i>		24.6	0.5	<0.0001		320	86

Table 1 (continued)

	Genotype	RNAi	Treatment	Mean lifespan	SE	P versus con/untreated	P versus wt	Sample size	Censor
	<i>ndx-4(ok1003)</i>	<i>isp-1</i>		30.1	0.5	<0.0001		240	23
		con		17.5	0.4		<0.0001	139	15
		<i>frh-1</i>		25.7	0.7	<0.0001	NS	137	42
	<i>nth-1(ok724)</i>	<i>isp-1</i>		30.8	1.8	<0.0001	0.0001	67	14
		con		19.7	0.4		NS	139	34
		<i>frh-1</i>		28.0	0.7	<0.0001	0.0008	140	32
	<i>ung-1(qa7600)</i>	<i>isp-1</i>		32.5	2.4	<0.0001	<0.0001	69	21
		con		21.3	0.4		0.0004	140	15
		<i>frh-1</i>		24.7	0.7	<0.0001	NS	140	40
	<i>xpa-1(ok698)</i>	<i>isp-1</i>		31.7	1.4	<0.0001	0.0396	70	13
		con		18.9	0.4		NS	140	16
		<i>frh-1</i>		23.8	0.6	<0.0001	NS	137	14
	Wild-type N2	<i>isp-1</i>		24.5	2.1	<0.0001	<0.0001	70	30
		con		16.7	0.4			140	9
		<i>frh-1</i>		23.9	0.7	<0.0001		136	26
	nT1	con		19.2	0.7		0.0025	138	17
		<i>frh-1</i>		23.9	0.6	0.0003	NS	135	20
	<i>atl-1(tm853)</i>	con		13.1	0.4		<0.0001	140	53
		<i>frh-1</i>		13.3	0.3	NS	<0.0001	146	55

In previous studies, we showed that reduced frataxin expression sensitizes mammalian cells to mitochondrial stress-induced apoptosis [43], indicating cells are unable to cope with additional mitochondrial stress, yet similar to partial frataxin depletion in worms, also mammalian cells clearly try to survive by activating protecting pathways such as autophagy or mitophagy [14,44]. In this context, the induction of specific DNA-damage protective and detoxification pathways can be seen as part of a hormetic response to moderate mitochondrial stress, which activates damage specific responses in a cell-non-autonomous manner, while other *Mit* phenotypes being concurrently mediated by alternative protective mechanisms (e.g., autophagy [14,44] or other DDR [17,23] and Borror *et al*, under revision). Consistent with this scenario, proliferating germ cells may specifically activate *brc-1/brd-1*-mediated repair in response to low levels of mitochondrial stress-induced DNA damage or replication stress. Yet, in the absence of these two genes, germ cells may attempt to repair DNA by activating non-homologous end-joining leading to increased lethality and cell death, thus suppressing the apoptotic protection elicited by reduced mitochondrial function. Accordingly, the observed unchanged apoptotic resistance of *frh-1*- and *isp-1*-depleted animals to cisplatin compared to other genotoxic insults could be explained by the presence of low level of mitochondrial stress-induced double-strand breaks, as it has been shown that cisplatinated DNA affects DNA repair [45]. Alternatively, the unaltered response to cisplatin-induced apoptosis could be ascribed by mitochondrial dysfunction inducing an hypoxia-like state [44], which were shown to enhance cisplatin pro-apoptotic effect [46]. Although in a different study we could not observe any obvious sign of DNA damage in response to mild mitochondrial stress (Borror *et al*, under revision), low levels of undetectable DNA damage or

replication stress could be caused by transient increase in reactive oxygen species (ROS) production during the period of germline expansion and/or as a consequence of the observed reduced PARP1 recruitment (Fig 4) due to NAD^+/NADH ratio imbalance [28,47]. ROS scavengers indeed prevent the lifespan extension elicited by MRC dysfunction [48], and a similar suppressive effect would be expected with NAD supplementation—as opposed to its lifespan-extending effects in wild-type animals [49] or in DNA-damage repair mutants [50] where the primary NAD defect could be instead ascribed to PARP overactivation. As an alternative to DNA damage, DDR could be induced by changes in chromatin structure [51], which have been also implicated in mitochondrial stress control of longevity [30,52]. Furthermore, in yeast, mitochondrial dysfunction leads to DDR activation via defective iron-sulfur cluster (ISC) biogenesis [53,54]. Different DNA repair genes which we found to mediate *isp-1* mutants phenotypes (e.g., DNA-glycosylases, helicases, nucleases [55–57]) rely on ISC, whose biogenesis is impaired by frataxin depletion [58,59] and could be similarly affected upon suppression of ISP-1, an ISC protein itself. Additional studies will be thus required to understand whether in *C. elegans* the protective germline DDR is uniquely induced by *isp-1* and *frh-1* depletion or whether it could be more generally triggered, and by which cell non-autonomous signals, following different types of mitochondrial stress. It will be also interesting to identify genes required upon mitochondrial stress to protect against different pro-apoptotic agents.

Our study also points to BRC/BRD-independent mechanisms regulating fertility and longevity in response to mitochondrial stress. Since an iron-starvation response mediates frataxin-depleted animal longevity [44], reduced cell proliferation due to iron depletion

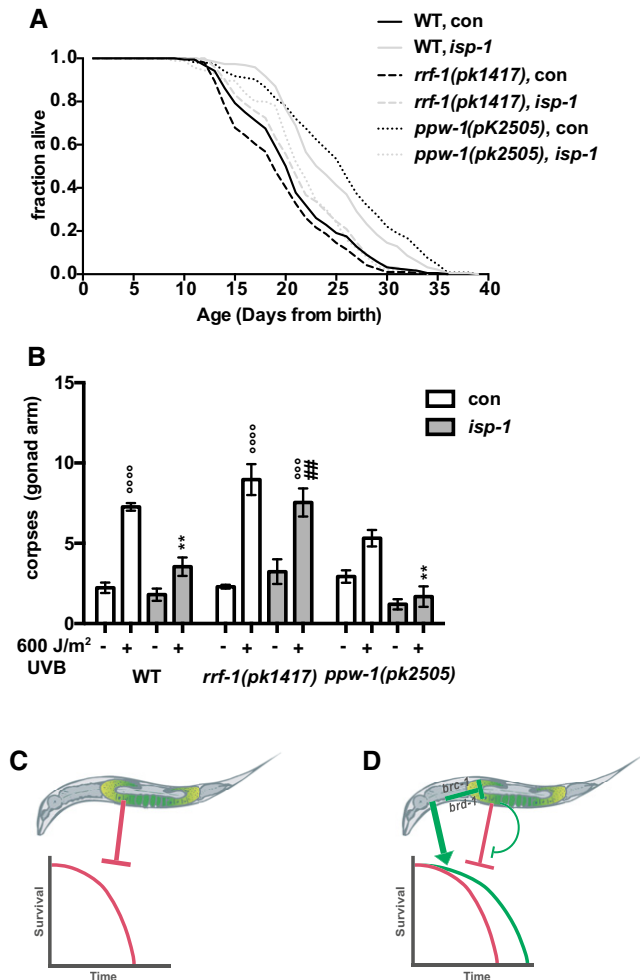


Figure 8. Mitochondrial stress mediates germline apoptosis and lifespan through different cell non-autonomous mechanisms.

- A** Kaplan-Meier survival curves of wild-type (WT) and, *rrf-1(pk1417)*, *ppw-1(pk2505)* strains fed bacteria transformed with either empty-vector (con) or with vector-expressing dsRNA against *isp-1*. Comparison between curves was done using the log-rank test, and the summary of the statistic is reported in Table 1.
- B** Quantification of apoptotic corpses in wild-type (WT) and *rrf-1(pk1417)*, *ppw-1(pk2505)* strains fed as (A) and left untreated or treated with 600 J/m² UVB.
- C** In the wild-type animals, under normal conditions a signal from the germline limits lifespan.
- D** Systemic mitochondrial stress concurrently triggers a pro-longevity signal from the soma (independent from the germline) and a cell-autonomous germline signal partially inhibiting the limiting signal from the gonad, ultimately resulting in significant lifespan extension in the wild-type and further extending lifespan in germline-less strains. Moreover, it induces a soma-to-germline signal that protects against IR-induced apoptosis in a *brc-1/brd-1*-dependent manner. In a germline-competent strain, somatic *isp-1* RNAi would only trigger the pro-longevity signal in the soma, which in the presence of the lifespan-limiting effects from the germline turns into detrimental effects on lifespan. When *isp-1* is instead only silenced in the germline, the anti-apoptotic effect is lost, while the absence of the pro-longevity signal from the soma and the partial suppression of the limiting signal in the germline would result in lifespan-extending effects, yet reduced compared to systemic MRC stress.

Data information: (B) Data are presented as mean \pm SEM, $N = 3$, 9–10 worms per replicate and condition ** $P < 0.01$ versus con; ## $P < 0.01$ versus WT; °°° $P < 0.00$ and °°°° $P < 0.0001$ versus untreated. Not significant if nothing is specified. Two-way ANOVA Tukey's multiple comparisons test.

[60–62] is likely the cause of *Mit* mutants altered fertility and smaller germline, two parameters which clearly reflect defective regulation of gonad formation. Thus, reduced germ-cell proliferation during larval development, a critical stage for the specification of *Mit* mutants' longevity [36,63], may be either associated with or causally involved in lifespan extension in response to mitochondrial stress. In support of a causal connection between reduced germ-cell proliferation and lifespan extension is the number of mitotic and meiotic genes required for *isp-1* mutants' longevity [23] and the tight crosstalk between cell proliferation and autophagy that could in turn modulate lifespan in response to mitochondrial stress [64–67]. Our data with the germline-less mutants and tissue-specific RNAi revealed a complex crosstalk between soma and the germline in the specification of *isp-1* longevity, thus opening the interesting possibility for a role of mitotic and meiotic regulatory genes on somatic maintenance and lifespan independent of their classical role in cell cycle regulation. While results from our screening unambiguously indicate a central role for DNA maintenance and detoxification genes in mediating *isp-1* survival, additional work is clearly required to identify those specifying longevity. Of special interest could be genes involved in nucleotide excision repair or suppressors of the *isp-1* developmental delay (such as *csb-1* or *atl-1*, Appendix Table S1; Fig EV4 and Borror *et al*, under revision). These genes could be triggered in a tissue-specific manner depending on the degree of MRC dysfunction in turn being more relevant for somatic maintenance and aging. One such gene, *cep-1*, which in the past we identified as suppressor of both lifespan extension and developmental delay upon moderate and severe mitochondrial dysfunction, respectively, is also up-regulated in frataxin-deficient cells [68]. However, here we find that the *cep-1*-dependent checkpoint is not affected by *frh-1* or *isp-1* silencing, indicating that *cep-1*/p53-regulated processes other than apoptosis or cell cycle arrest are activated in a tissue-specific manner in response to MRC dysfunction to extend lifespan. Obvious candidates would be autophagy [14], metabolic pathways, or *cep-1* functions related to other p53 family members, p63 and p73 (stress response, development, and differentiation [69,70]). Considering the heterogeneity of symptoms associated with the presentation of the different human mitochondrial disorders, tissue-specific responses triggered upon MRC dysfunction may point toward novel potential pathogenic mechanisms and targeted therapeutic approaches for this wide class of diseases, which to date have no effective cure.

Contrasting findings were previously reported on physiological germline apoptosis in the long-lived *isp-1(qm150)* *Mit* mutant [18,71]. This discrepancy is most likely ascribed to the different techniques used to score the very low numbers of apoptotic corpses under physiological conditions, as we also obtained non-identical results in basal conditions using different assays. Nonetheless, moderate RNAi-mediated mitochondrial stress consistently and significantly suppressed genotoxic stress-induced apoptosis in a time- and dose-dependent manner. Lack of the anti-apoptotic *ced-9* gene clearly affects both germ-cell apoptosis and lifespan extension upon mitochondrial stress, while loss of *brc-1* and *brd-1* impinged on apoptosis but inconsistently affected animal longevity. These results are in agreement with previous reports showing that lack of another apoptosis-regulatory gene, *egl-1*, does not mediate *Mit* mutants' lifespan extension [7,23] and indicate that apoptosis resistance is not required per se for animal longevity. Thus, *ced-9* might regulate longevity through apoptosis- or germline-independent

functions. Besides its classical role as an anti-apoptotic protein, the mammalian CED-9 ortholog BCL-2 and its family members play a role in several other important biological processes as diverse as mitochondrial physiology (e.g., mitophagy, morphology, metabolism), nuclear functions (e.g., cell cycle, DNA repair), and cell homeostasis (e.g., autophagy, lipid metabolism) [72], which interestingly have been all associated and/or causally involved in *Mit* mutants longevity [14,23,24]. In *C. elegans*, autophagy is induced as a protective mechanism against mitochondrial stress [14,44] and to counteract embryonic lethality and apoptosis in different contexts [73,74]. Therefore, *ced-9*-regulation of autophagy may help revealing further insight into its role in *Mit* mutants' control of DDR and longevity. Moreover, whether and how *ced-9* cooperates with *brc-1* and *brd-1* to modulate germline cell death processes upon mitochondrial stress remain to be investigated. Interestingly, mammalian BRCA1 and BARD1 were shown to interact with Bcl2 and mitochondria in turn regulating responses to DNA-damaging agents [75–77].

The induction of a hormetic protective response to mitochondrial perturbation is a common feature of both RNAi- and genetic-derived *Mit* mutants, which include their increased resistance to stress and altered neuronal functionality [13,78–80] as well as the induction of similar DDR regulatory genes and the requirement of CEP-1/p53 for their lifespan extension [7,17,18,23]. Yet, RNAi- and genetic-derived *Mit* mutants also differ under some extent such as developmental rate [36,81], content of ROS [36,82], and requirement of AMP kinases for their lifespan extension [7,26]. Our study brings further evidence to this scenario. On the one hand, we observed that similar to the *isp-1* genetic mutant [71] also *isp-1* RNAi-depleted animal has a reduced number of mitotic germ cells. On the other hand, we show that while survival of *isp-1* genetic mutants is affected by silencing of DNA-maintenance genes, *isp-1* (and *frh-1*) RNAi animals were still able to extend lifespan in knockout strains for some of the same DDR genes. These differences could either reflect the efficiency in gene knock-down versus knockout or acute versus chronic habituation to stress (mitochondrial or genotoxic) or most likely indicate that RNAi- and genetic-mediated *Mit* phenotypes are in part specified by different underlying molecular mechanisms. Regardless, together with previous findings showing that DDR genes mediate *Mit* mutants longevity [7,17,18,23] and that DDR mutants have altered mitochondrial metabolism [40,50,83–85], our data reinforce the notion that a tight crosstalk exists between mitochondria and the nucleus, which must be preserved and finely regulated to sustain organismal fitness. In conclusion, we showed that in animals with reduced mitochondrial activity, the mechanisms activated to safeguard germ cells against genotoxic stress are uncoupled from those required for somatic fitness, a very likely process from an evolutionarily point of view.

Materials and Methods

Nematode strains

All strains were cultured according to standard conditions. Strains utilized were as follows: N2 (wild-type), MQ887 [*isp-1(qm150)* IV], CL2166 [dvIs19[pAF15(*gst-4::gfp::NLS*)] III], CB3203 [*ced-1(e1735)* I], DW102 [*brc-1(tm1145)*], RB1209 [*brc-1(ok1261)* III], DW103 [*brd-1(dw1)*], RB1426 [*brd-1(ok1623)* III], VC655 [*brd-1(gk297)* III], and *ced-9(n1653ts)* (kind gift from A. Gartner Lab). MD701 [*lim-7p::*

ced-1::GFP + lin-15(+)], RB1054 [*ndx-4(ok1003)*], RB877 [*nth-1(ok724)*], [*ung-1(qa7600)*], RB864 [*xpa-1(ok698)*], NL2550 [*(ppw-1(pk2505))*], NL2098 *rrf-1(pk1417)*, MQ887 previously crossed with CL2166 to obtain TJ564 [*isp-1(qm150)*; pAF15(*gst-4p::gfp::NLS*)], was used, together with its respective control, for the RNAi screening. TJ564 was further crossed with *cep-1(gk138)* (outcrossed 10x) to obtain NV7 [*gst-4p::gfp::NLS*; *isp-1(qm150)*], NV11 [*gst-4p::gfp::NLS*], NV10 [*gst-4p::gfp::NLS*; *cep-1(gk138)*], and NV15 [*gst-4p::gfp::isp-1(qm150)*; *cep-1(gk138)*].

Feeding RNAi

RNAi feeding techniques was performed as we previously described [7]. In all the experiments present in this study, animals were fed for three consecutive generations with bacteria expressing *frh-1IV* dsRNA, which target the entire *frh-1* CDS [14]. *isp-1* RNAi was used at the final concentration of 1:15 [36].

Lifespan and statistical analysis

Survival curves and statistical analyses were carried out as we previously described [44]. Briefly, survival analysis of all lifespan experiments started from hatching and was scored at 20°C using synchronous populations of 60–80 animals per curve unless otherwise indicated. Animals were scored as dead or alive and transferred every day on fresh plates during the fertile period, and then every other day until death. Worms were considered dead when they stop pharyngeal pumping and responding to touch. Worms that die because of internal bagging, desiccation due to crawling on the edge of the plates, or gonad extrusion were scored as censored and included in the statistical analysis until the day of censoring. Data from survival assays are summarized in Table 1. Figures display survival curves of pooled populations utilized for statistical analysis.

Western blotting

Western blot experiments and analysis were performed as previously described [14]. Anti BRD-1 antibody was kindly provided by Simon Boulton [42]. Anti-Tub 1:20,000 (DM1A) (#T9026 Sigma).

Quantification of mitotic germ cells

Mitotic germ-cell nuclei were counted, 24 h after the L4 larval stage, in isolated adult germlines stained with the DNA-intercalating dye 4',6-diamidino-2-phenylindole (DAPI). The mitotic zone extends from the distal tip of the gonad arm and continues until the appearance of nuclei with crescent-shape DNA morphology, characteristic of leptotene/zygotene (transition zone) germ cells as defined previously [86]. Differential interference contrast (DIC) microscopy (Zeiss Axio Imager M1—Carl Zeiss, Inc.) was used to estimate size of mitotic region by counting nuclei on each focal plane.

5-Ethynyl-2'-deoxyuridine (EdU) labeling and staining

EdU labeling and detection were made as previously described [87]. MG1693 bacteria that incorporated 5-ethynyl-2-deoxyuridine (EdU, Invitrogen) were seeded on plates 1 day before the experiment. EdU was used at the final concentration of 10 μ M. Synchronized

animals, 24 h after the L4 larval stage, were transferred on plates containing EdU for 1 h before transferring them back to normal NGM plates. Dissection of gonads was done at 0 and 24 h directly after labeling, and EdU detection was performed using Click-IT EdU Alexa Fluor-555 labeling kit (Invitrogen). All samples were analyzed using a PerkinElmer spinning disk confocal microscope and Velocity imaging software. EdU-positive nuclei were scored throughout the proliferative zone by assaying multiple focal planes.

Quantification of germ-cell apoptosis

Apoptotic germ-cell corpses in the meiotic prophase region of adult hermaphrodite germ lines were scored using DIC microscopy (Zeiss Axio Imager M1—Carl Zeiss, Inc.), as highly refractile structures [88]. In some experiments, apoptotic corpses were visualized using the *ced-1::gfp* strain under differential interference contrast (DIC) microscopy using a Zeiss Axiovert 200 M inverted microscope with x100 Plan-Apochromat 1.45 NA objective. Nematodes were anesthetized with 15–30 mM sodium azide in M9 buffer and mounted on 2% agar pads.

UVB irradiation

UVB irradiation of synchronized L4 larval stage animals was performed with a UV 236 B (Waldmann Medizintechnik) device equipped with UV6 lamp, and germ-cell death was measured at the indicated time points.

Ionizing radiation

Synchronized L4 hermaphrodites were irradiated with 125 Gy of IR in M9 buffer in a MDS Nordion Gammacell 3000 Elan.

UVC irradiation

UVC irradiation of synchronized L4 larval stage animals or 1-day adults was performed with a Bio-Link Crosslinker device using the indicated J/m².

Cisplatin

Cisplatin treatment was performed on L4 larval stage animals for 24 h in S-Medium (liquid medium) in a 12-well plate on a rotating plate in the dark followed by 24-h recovery time before the determination of apoptotic corpse using a BX43 fluorescence microscope (Olympus).

Hydroxyurea (HU)

L4 worms were treated for 16 h with a final concentration of hydroxyurea (Sigma-Aldrich, H8627) of 0, 25 and 40 mM. HU was spotted at the final concentration directly on the plates the day before the treatment. And the fertility and fecundity were scored as described in *Radiation sensitivity assay*.

Quantification of somatic cell apoptosis

Extra corpses in the head of *ced-1(e1735)* corpse engulfment-defective animals at the L1 larval stage were counted using DIC microscopy (Zeiss Axio Imager M1—Carl Zeiss, Inc.) [89].

Radiation sensitivity assay

L4 stage worms were treated with the indicated DNA-damaging agents. Twenty-four hours after treatment, three P0 worms for each condition were placed in NGM plates containing a freshly seeded 1-cm-diameter bacterial lawn in the center of the dish and allowed to lay eggs for a period of 3 h. Adult worms were removed, and eggs were counted with a dissection microscope. Forty-eight hours later, hatched F1 larvae and dead embryos were scored. Fecundity and fertility rates were calculated by combining the numbers of laid and hatched eggs. Experiments were done in triplicate.

Immunostaining

Worms were dissected on poly-L-lysine-coated slides in egg buffer (Edgar, 1995) supplemented with 0.1% Tween-20 and 20 mM sodium azide. Germlines were fixed in 3.7% formaldehyde for 2 min at room temperature (RT) followed by freeze-cracking by immersion in liquid nitrogen. Post-fixation was done in methanol at –20°C for 1 min followed by two washes in PBS + 0.1% Tween-20 (PBST). Blocking was performed by incubating the samples in 10% donkey serum in PBST for 30 min. Primary antibody was diluted in 10% donkey serum in PBST and allowed to bind at 4°C overnight in a humid chamber. Samples were washed two times for 10 min in PBST. Binding of secondary antibodies was performed for 2 h at RT with antibodies diluted in PBST. After washing three times for 10 min in PBST, the samples were mounted in mounting medium (90% glycerol, 20 mM Tris at pH 8.0, 1 mg/ml p-phenylenediamine). Pictures were taken with a Zeiss Axio Imager Z1 (Carl Zeiss, Inc.). Primary antibodies for immunofluorescence were used as follows: rat anti-RPA-1 1:200 (kindly donated by Anton Gartner from the University of Dundee), rabbit anti-histone H3 (pSer-10) 1:400 (Santa Cruz Biotechnology, Inc., Santa Cruz, USA), rabbit anti-CDK1 (pTyr-15) 1:100 (VWR, Oslo, Norway), and rabbit anti-PARP1 (46D11) 1:1,000 (mAb#9532, Cell Signaling). The following secondary antibodies were used: Cy3-conjugated anti-rabbit (Sigma-Aldrich, St. Louis, USA) 1:2,000 for detection of anti-PARP1 and 1:1,000 for detection of CDK-1, respectively, and 1:1,000 Alexa 488-conjugated anti-rat (Invitrogen, Carlsbad, USA).

Genetic screen

The DDR RNAi bacterial feeding library consists of 201 DNA maintenance-related genes which were sub-cloned from the Ahinger *C. elegans* RNAi Collection (Source Bioscience) into three 96-well stock plates. Genes related to DNA maintenance were selected based on previously published paper or identified using WormMine (www.wormbase.org). The phenotype of the *Pgst4::gfp* and *isp1(qm150);Pgst4::gfp* strains was monitored every day for two consecutive generations on every RNAi clone. Differences in viability (let), development (dev), fertility (fer or ste), and *gst-4* expression (gfp) were registered in three independent rounds of screening. After three rounds of screening, we excluded those clones that (i) gave no phenotype, (ii) similarly affected both strains, and (iii) gave inconsistent results. Thus, clones that 2 out of 3 rounds of screening specifically affected *isp-1* mutants were shortlisted for sequencing and validation on other two rounds of screening. Only those clones that

consistently affected *isp-1* mutants in at least one phenotype other than the *gst-4* expression were then selected for further analysis.

Expanded View for this article is available online.

Acknowledgements

Most nematode strains utilized in this work were provided by the Caenorhabditis Genetics Center, funded by the NIH Office of Research Infrastructure Programs (P40 OD010440). Other strains were kindly provided by Anton Gartner, *ced-9(n1653ts)*, and Hilde Nilsen, RB864 [*xpa-1(ok698)*], RB1054 [*ndx-4(ok1003)*], RB877 [*nth-1(ok724)*], and *ung-1(qa7600)*. This work was financially supported by funding to N.V.: Associazione Italiana per la Ricerca sul Cancro (AIRC) (MFAG11509), the Research Commission of the Medical Faculty of the Heinrich-Heine-University (Grant no. 9772559), and the Deutsche Forschungsgemeinschaft (VE663/3-1) and H.N.: The South East Norway Regional Health Authority (Project no. 2015029). A.T. was in part supported by a short-term EMBO fellowship (ASTF 132-2011). The authors would like to thank the "GENIE" COST Action BM1408.

Author contributions

AT, ASH, and HK performed most of the experiments; ASH, SM, and SH performed some of the experiments; ASH, AT, and NV analyzed the data; ASH prepared all the figures and helped writing the manuscript; AT helped writing the manuscript and assembling the figures; SLR and TEJ were involved in the DDR screening design and financial support; HCR financially supported AT during the revision of the manuscript; BS and HN supervised and financially supported part of the study and provided their valuable insight during manuscript writing; NV conceptualized, designed, coordinated and financially supported the study, and wrote the manuscript.

Conflict of interest

The authors declare that they have no conflict of interest.

References

- Ermolaeva MA, Dakhovnik A, Schumacher B (2015) Quality control mechanisms in cellular and systemic DNA damage responses. *Ageing Res Rev* 23: 3–11
- Vermeij WP, Hoeijmakers JH, Pothof J (2016) Genome integrity in aging: human syndromes, mouse models, and therapeutic options. *Annu Rev Pharmacol Toxicol* 56: 427–445
- Lopez-Otin C, Blasco MA, Partridge L, Serrano M, Kroemer G (2013) The hallmarks of aging. *Cell* 153: 1194–1217
- Lionaki E, Markaki M, Tavernarakis N (2013) Autophagy and ageing: insights from invertebrate model organisms. *Ageing Res Rev* 12: 413–428
- Shore DE, Ruvkun G (2013) A cytoprotective perspective on longevity regulation. *Trends Cell Biol* 23: 409–420
- Johnson TE, Cypser J, de Castro E, de Castro S, Henderson S, Murakami S, Rikke B, Tedesco P, Link C (2000) Gerontogenes mediate health and longevity in nematodes through increasing resistance to environmental toxins and stressors. *Exp Gerontol* 35: 687–694
- Ventura N, Rea SL, Schiavi A, Torgovnick A, Testi R, Johnson TE (2009) p53/CEP-1 increases or decreases lifespan, depending on level of mitochondrial bioenergetic stress. *Aging Cell* 8: 380–393
- Ermolaeva MA, Segref A, Dakhovnik A, Ou HL, Schneider JI, Utermohlen O, Hoppe T, Schumacher B (2013) DNA damage in germ cells induces an innate immune response that triggers systemic stress resistance. *Nature* 501: 416–420
- Melo JA, Ruvkun G (2012) Inactivation of conserved *Caenorhabditis elegans* genes engages pathogen- and xenobiotic-associated defenses. *Cell* 149: 452–466
- Shore DE, Carr CE, Ruvkun G (2012) Induction of cytoprotective pathways is central to the extension of lifespan conferred by multiple longevity pathways. *PLoS Genet* 8: e1002792
- Rea SL (2005) Metabolism in the *Caenorhabditis elegans* Mit mutants. *Exp Gerontol* 40: 841–849
- Ventura N, Rea SL, Testi R (2006) Long-lived *Caenorhabditis elegans* mitochondrial mutants as a model for human mitochondrial-associated diseases. *Exp Gerontol* 41: 974–991
- Butler JA, Ventura N, Johnson TE, Rea SL (2010) Long-lived mitochondrial (Mit) mutants of *Caenorhabditis elegans* utilize a novel metabolism. *FASEB J* 24: 4977–4988
- Schiavi A, Torgovnick A, Kell A, Megalou E, Castelein N, Guccini I, Marzocchella L, Gelino S, Hansen M, Malisan F et al (2013) Autophagy induction extends lifespan and reduces lipid content in response to frataxin silencing in *Caenorhabditis elegans*. *Exp Gerontol* 48: 191–201
- Durieux J, Wolff S, Dillin A (2011) The cell-non-autonomous nature of electron transport chain-mediated longevity. *Cell* 144: 79–91
- Houtkooper RH, Mouchiroud L, Ryu D, Moullan N, Katsyuba E, Knott G, Williams RW, Auwerx J (2013) Mitonuclear protein imbalance as a conserved longevity mechanism. *Nature* 497: 451–457
- Torgovnick A, Schiavi A, Testi R, Ventura N (2010) A role for p53 in mitochondrial stress response control of longevity in *Caenorhabditis elegans*. *Exp Gerontol* 45: 550–557
- Baruah A, Chang H, Hall M, Yuan J, Gordon S, Shtessel LL, Yee C, Hekimi S, Derry WB et al (2014) CEP-1, the *Caenorhabditis elegans* p53 homolog, mediates opposing longevity outcomes in mitochondrial electron transport chain mutants. *PLoS Genet* 10: e1004097
- Walter L, Baruah A, Chang HW, Pace HM, Lee SS (2011) The homeobox protein CEH-23 mediates prolonged longevity in response to impaired mitochondrial electron transport chain in *Caenorhabditis elegans*. *PLoS Biol* 9: e1001084
- Khan MH, Ligon M, Hussey LR, Hufnal B, Farber R II, Munkacsy E, Rodriguez A, Dillow A, Kahlig E, Rea SL (2013) TAF-4 is required for the life extension of *isp-1*, *clk-1* and *tpk-1* Mit mutants. *Aging* 5: 741–758
- Lapierre LR, De Magalhaes Filho CD, McQuary PR, Chu CC, Visvikis O, Chang JT, Gelino S, Ong B, Davis AE, Irazoqui JE et al (2013) The TFEB orthologue HLH-30 regulates autophagy and modulates longevity in *Caenorhabditis elegans*. *Nat Commun* 4: 2267
- Lee SJ, Hwang AB, Kenyon C (2010) Inhibition of respiration extends *Caenorhabditis elegans* life span via reactive oxygen species that increase HIF-1 activity. *Curr Biol* 20: 2131–2136
- Yee C, Yang W, Hekimi S (2014) The intrinsic apoptosis pathway mediates the pro-longevity response to mitochondrial ROS in *Caenorhabditis elegans*. *Cell* 157: 897–909
- Toth ML, Sigmund T, Borsos E, Barna J, Erdelyi P, Takacs-Vellai K, Orosz L, Kovacs AL, Csikos G, Sass M et al (2008) Longevity pathways converge on autophagy genes to regulate life span in *Caenorhabditis elegans*. *Autophagy* 4: 330–338
- Munkacsy E, Khan MH, Lane RK, Borror MB, Park JH, Bokov AF, Fisher AL, Link CD, Rea SL (2016) DLK-1, SEK-3 and PMK-3 are required for the life extension induced by mitochondrial bioenergetic disruption in *Caenorhabditis elegans*. *PLoS Genet* 12: e1006133

26. Curtis R, O'Connor G, DiStefano PS (2006) Aging networks in *Caenorhabditis elegans*: AMP-activated protein kinase (aak-2) links multiple aging and metabolism pathways. *Aging Cell* 5: 119–126
27. Chang HW, Pisano S, Chaturvedi A, Chen J, Gordon S, Baruah A, Lee SS (2017) Transcription factors CEP-1/p53 and CEH-23 collaborate with AAK-2/AMPK to modulate longevity in *Caenorhabditis elegans*. *Aging Cell* 16: 814–824
28. Mishur RJ, Khan M, Munkacsy E, Sharma L, Bokov A, Beam H, Radetskaya O, Borrer M, Lane R, Bai Y et al (2016) Mitochondrial metabolites extend lifespan. *Aging Cell* 15: 336–348
29. Merkwirth C, Jovaisaite V, Durieux J, Matilainen O, Jordan SD, Quiros PM, Steffen KK, Williams EG, Mouchiroud L, Tronnes SU et al (2016) Two conserved histone demethylases regulate mitochondrial stress-induced longevity. *Cell* 165: 1209–1223
30. Tian Y, Garcia G, Bian Q, Steffen KK, Joe L, Wolff S, Meyer BJ, Dillin A (2016) Mitochondrial stress induces chromatin reorganization to promote longevity and UPR(mt). *Cell* 165: 1197–1208
31. Cristina D, Cary M, Lunceford A, Clarke C, Kenyon C (2009) A regulated response to impaired respiration slows behavioral rates and increases lifespan in *Caenorhabditis elegans*. *PLoS Genet* 5: e1000450
32. Dues DJ, Schaar CE, Johnson BK, Bowman MJ, Winn ME, Senchuk MM, Van Raamsdonk JM (2017) Uncoupling of oxidative stress resistance and lifespan in long-lived isp-1 mitochondrial mutants in *Caenorhabditis elegans*. *Free Radic Biol Med* 108: 362–373
33. Ventura N, Rea S, Henderson ST, Condo I, Johnson TE, Testi R (2005) Reduced expression of frataxin extends the lifespan of *Caenorhabditis elegans*. *Aging Cell* 4: 109–112
34. Derry WB, Putzke AP, Rothman JH (2001) *Caenorhabditis elegans* p53: role in apoptosis, meiosis, and stress resistance. *Science* 294: 591–595
35. Schumacher B, Hofmann K, Boulton S, Gartner A (2001) The *Caenorhabditis elegans* homolog of the p53 tumor suppressor is required for DNA damage-induced apoptosis. *Curr Biol* 11: 1722–1727
36. Rea SL, Ventura N, Johnson TE (2007) Relationship between mitochondrial electron transport chain dysfunction, development, and life extension in *Caenorhabditis elegans*. *PLoS Biol* 5: e259
37. Stergiou L, Hengartner MO (2004) Death and more: DNA damage response pathways in the nematode *Caenorhabditis elegans*. *Cell Death Differ* 11: 21–28
38. Stergiou L, Doukometzidis K, Sandoel A, Hengartner MO (2007) The nucleotide excision repair pathway is required for UV-C-induced apoptosis in *Caenorhabditis elegans*. *Cell Death Differ* 14: 1129–1138
39. Kim HM, Colaiacovo MP (2015) DNA damage sensitivity assays in *Caenorhabditis elegans*. *Bio Protoc* 5: e1487
40. Arczewska KD, Tomazella GG, Lindvall JM, Kassahun H, Maglioni S, Torgounick A, Henriksson J, Matilainen O, Marquis BJ, Nelson BC et al (2013) Active transcriptomic and proteomic reprogramming in the *Caenorhabditis elegans* nucleotide excision repair mutant xpa-1. *Nucleic Acids Res* 41: 5368–5381
41. Ventura N, Rea SL (2007) *Caenorhabditis elegans* mitochondrial mutants as an investigative tool to study human neurodegenerative diseases associated with mitochondrial dysfunction. *Biotechnol J* 2: 584–595
42. Boulton SJ, Martin JS, Polanowska J, Hill DE, Gartner A, Vidal M (2004) BRCA1/BARD1 orthologs required for DNA repair in *Caenorhabditis elegans*. *Curr Biol* 14: 33–39
43. Condo I, Ventura N, Malisan F, Tomassini B, Testi R (2006) A pool of extramitochondrial frataxin that promotes cell survival. *J Biol Chem* 281: 16750–16756
44. Schiavi A, Maglioni S, Palikaras K, Shaik A, Strappazzon F, Brinkmann V, Torgounick A, Castelein N, De Henau S, Braeckman BP et al (2015) Iron-starvation-induced mitophagy mediates lifespan extension upon mitochondrial stress in *Caenorhabditis elegans*. *Curr Biol* 25: 1810–1822
45. Diggle CP, Bentley J, Knowles MA, Kiltie AE (2005) Inhibition of double-strand break non-homologous end-joining by cisplatin adducts in human cell extracts. *Nucleic Acids Res* 33: 2531–2539
46. Schwerdt G, Freudinger R, Schuster C, Weber F, Thews O, Gekle M (2005) Cisplatin-induced apoptosis is enhanced by hypoxia and by inhibition of mitochondria in renal collecting duct cells. *Toxicol Sci* 85: 735–742
47. Butler JA, Mishur RJ, Bhaskaran S, Rea SL (2013) A metabolic signature for long life in the *Caenorhabditis elegans* Mit mutants. *Aging Cell* 12: 130–138
48. Yang W, Hekimi S (2010) A mitochondrial superoxide signal triggers increased longevity in *Caenorhabditis elegans*. *PLoS Biol* 8: e1000556
49. Mouchiroud L, Houtkooper RH, Moullan N, Katsyuba E, Ryu D, Canto C, Mottis A, Jo YS, Viswanathan M, Schoonjans K et al (2013) The NAD(+)/sirtuin pathway modulates longevity through activation of mitochondrial UPR and FOXO signaling. *Cell* 154: 430–441
50. Fang EF, Scheibye-Knudsen M, Brace LE, Kassahun H, SenGupta T, Nilsen H, Mitchell JR, Croteau DL, Bohr VA (2014) Defective mitophagy in XPA via PARP-1 hyperactivation and NAD(+)/SIRT1 reduction. *Cell* 157: 882–896
51. Bakkenist CJ, Kastan MB (2003) DNA damage activates ATM through intermolecular autophosphorylation and dimer dissociation. *Nature* 421: 499–506
52. Monaghan RM, Barnes RG, Fisher K, Andreou T, Rooney N, Poulin GB, Whitmarsh AJ (2015) A nuclear role for the respiratory enzyme CLK-1 in regulating mitochondrial stress responses and longevity. *Nat Cell Biol* 17: 782–792
53. Pijuan J, Maria C, Herrero E, Belli G (2015) Impaired mitochondrial Fe-S cluster biogenesis activates the DNA damage response through different signaling mediators. *J Cell Sci* 128: 4653–4665
54. Veatch JR, McMurray MA, Nelson ZW, Gottschling DE (2009) Mitochondrial dysfunction leads to nuclear genome instability via an iron-sulfur cluster defect. *Cell* 137: 1247–1258
55. Fuss JO, Tsai CL, Ishida JP, Tainer JA (2015) Emerging critical roles of Fe-S clusters in DNA replication and repair. *Biochim Biophys Acta* 1853: 1253–1271
56. Wu Y, Brosh RM Jr (2012) DNA helicase and helicase-nuclease enzymes with a conserved iron-sulfur cluster. *Nucleic Acids Res* 40: 4247–4260
57. Lukianova OA, David SS (2005) A role for iron-sulfur clusters in DNA repair. *Curr Opin Chem Biol* 9: 145–151
58. Stemmler TL, Lesuisse E, Pain D, Dancis A (2010) Frataxin and mitochondrial FeS cluster biogenesis. *J Biol Chem* 285: 26737–26743
59. Rouault TA, Tong WH (2008) Iron-sulfur cluster biogenesis and human disease. *Trends Genet* 24: 398–407
60. Puig S, Ramos-Alonso L, Romero AM, Martinez-Pastor MT (2017) The elemental role of iron in DNA synthesis and repair. *Metallomics* 9: 1483–1500
61. Zhang C (2014) Essential functions of iron-requiring proteins in DNA replication, repair and cell cycle control. *Protein & cell* 5: 750–760
62. Yu Y, Kovacevic Z, Richardson DR (2007) Tuning cell cycle regulation with an iron key. *Cell Cycle* 6: 1982–1994
63. Dillin A, Hsu AL, Arantes-Oliveira N, Lehrer-Graiwer J, Hsin H, Fraser AG, Kamath RS, Ahringer J, Kenyon C (2002) Rates of behavior and aging

- specified by mitochondrial function during development. *Science* 298: 2398–2401
64. Lapiere LR, Gelino S, Melendez A, Hansen M (2011) Autophagy and lipid metabolism coordinately modulate life span in germline-less *Caenorhabditis elegans*. *Curr Biol* 21: 1507–1514
 65. Wang MC, O'Rourke EJ, Ruvkun G (2008) Fat metabolism links germline stem cells and longevity in *Caenorhabditis elegans*. *Science* 322: 957–960
 66. Cianfanelli V, Fuoco C, Lorente M, Salazar M, Quondamatteo F, Gherardini PF, De Zio D, Nazio F, Antonioli M, D'Orazio M et al (2015) AMBRA1 links autophagy to cell proliferation and tumorigenesis by promoting c-Myc dephosphorylation and degradation. *Nat Cell Biol* 17: 20–30
 67. Shaik A, Schiavi A, Ventura N (2016) Mitochondrial autophagy promotes healthy aging. *Cell Cycle* 15: 1805–1806
 68. Guccini I, Serio D, Condo I, Rufini A, Tomassini B, Mangiola A, Maira G, Anile C, Fina D, Pallone F et al (2011) Frataxin participates to the hypoxia-induced response in tumors. *Cell Death Dis* 2: e123
 69. Dotsch V, Bernassola F, Coutandin D, Candi E, Melino G (2010) p63 and p73, the ancestors of p53. *Cold Spring Harb Perspect Biol* 2: a004887
 70. Levvero M, De Laurenzi V, Costanzo A, Gong J, Wang JY, Melino G (2000) The p53/p63/p73 family of transcription factors: overlapping and distinct functions. *J Cell Sci* 113(Pt 10): 1661–1670
 71. Pinkston JM, Garigan D, Hansen M, Kenyon C (2006) Mutations that increase the life span of *Caenorhabditis elegans* inhibit tumor growth. *Science* 313: 971–975
 72. Gross A, Katz SG (2017) Non-apoptotic functions of BCL-2 family proteins. *Cell Death Differ* 24: 1348–1358
 73. SenGupta T, Torgersen ML, Kassahun H, Vellai T, Simonsen A, Nilsen H (2013) Base excision repair AP endonucleases and mismatch repair act together to induce checkpoint-mediated autophagy. *Nat Commun* 4: 2674
 74. Takacs-Vellai K, Vellai T, Puoti A, Passannante M, Wicky C, Streit A, Kovacs AL, Muller F (2005) Inactivation of the autophagy gene bec-1 triggers apoptotic cell death in *Caenorhabditis elegans*. *Curr Biol* 15: 1513–1517
 75. Laulier C, Barascu A, Guirouilh-Barbat J, Pennarun G, Le Chalony C, Chevalier F, Palierne G, Bertrand P, Verbavatz JM, Lopez BS (2011) Bcl-2 inhibits nuclear homologous recombination by localizing BRCA1 to the endomembranes. *Cancer Res* 71: 3590–3602
 76. Brodie KM, Henderson BR (2010) Differential modulation of BRCA1 and BARD1 nuclear localisation and foci assembly by DNA damage. *Cell Signal* 22: 291–302
 77. Tembe V, Henderson BR (2007) BARD1 translocation to mitochondria correlates with Bax oligomerization, loss of mitochondrial membrane potential, and apoptosis. *J Biol Chem* 282: 20513–20522
 78. Maglioni S, Schiavi A, Runci A, Shaik A, Ventura N (2014) Mitochondrial stress extends lifespan in *Caenorhabditis elegans* through neuronal hormesis. *Exp Gerontol* 56: 89–98
 79. Matsuura T, Suzuki S, Musashino A, Kanno R, Ichinose M (2009) Retention time of attenuated response to diacetyl after pre-exposure to diacetyl in *Caenorhabditis elegans*. *J Exp Zool A Ecol Genet Physiol* 311: 483–495
 80. Lee SS, Lee RY, Fraser AG, Kamath RS, Ahringer J, Ruvkun G (2003) A systematic RNAi screen identifies a critical role for mitochondria in *Caenorhabditis elegans* longevity. *Nat Genet* 33: 40–48
 81. Feng J, Bussiere F, Hekimi S (2001) Mitochondrial electron transport is a key determinant of life span in *Caenorhabditis elegans*. *Dev Cell* 1: 633–644
 82. Yang W, Hekimi S (2010) Two modes of mitochondrial dysfunction lead independently to lifespan extension in *Caenorhabditis elegans*. *Aging Cell* 9: 433–447
 83. Gomes AP, Price NL, Ling AJ, Moslehi JJ, Montgomery MK, Rajman L, White JP, Teodoro JS, Wrann CD, Hubbard BP et al (2013) Declining NAD(+) induces a pseudohypoxic state disrupting nuclear-mitochondrial communication during aging. *Cell* 155: 1624–1638
 84. Fang EF, Scheibye-Knudsen M, Chua KF, Mattson MP, Croteau DL, Bohr VA (2016) Nuclear DNA damage signalling to mitochondria in ageing. *Nat Rev Mol Cell Biol* 17: 308–321
 85. Kassahun H, SenGupta T, Schiavi A, Maglioni S, Skjeldam HK, Arczewska K, Brockway NL, Estes S, Eide L, Ventura N et al (2018) Constitutive MAP-kinase activation suppresses germline apoptosis in NTH-1 DNA glycosylase deficient *Caenorhabditis elegans*. *DNA Repair* 61: 46–55
 86. Crittenden SL, Leonhard KA, Byrd DT, Kimble J (2006) Cellular analyses of the mitotic region in the *Caenorhabditis elegans* adult germ line. *Mol Biol Cell* 17: 3051–3061
 87. Fox PM, Vought VE, Hanazawa M, Lee MH, Maine EM, Schedl T (2011) Cyclin E and CDK-2 regulate proliferative cell fate and cell cycle progression in the *Caenorhabditis elegans* germline. *Development* 138: 2223–2234
 88. Gartner A, MacQueen AJ, Villeneuve AM (2004) Methods for analyzing checkpoint responses in *Caenorhabditis elegans*. *Methods Mol Biol* 280: 257–274
 89. Hedgecock EM, Sulston JE, Thomson JN (1983) Mutations affecting programmed cell deaths in the nematode *Caenorhabditis elegans*. *Science* 220: 1277–1279